IN SEARCH OF THE PHYSICS: NASA's APPROACH TO AIRFRAME NOISE

Michele G. Macaraeg, David P. Lockard, and Craig L. Streett
Aerodynamics, Aerothermodynamics, and Acoustics Competency
NASA Langley Research Center
Hampton, VA, 23681-2199 USA

Abstract

An extensive numerical and experimental study of airframe noise mechanisms associated with a subsonic high-lift system has been performed at NASA Langley Research Center (LaRC). Investigations involving both steady and unsteady computations and experiments on small-scale models with part-span flaps and full-span flaps are presented. Both surface (steady and unsteady pressure measurements, hot films, oil flows, pressure sensitive paint) and off-surface (5 hole-probe, particle-imaged velocimetry, laser velocimetry, laser light sheet measurements) were taken in the LaRC Quiet Flow Facility (QFF) and several hard-wall tunnels. Experiments in the Low Turbulence Pressure Tunnel (LTPT) included Reynolds number variations up to flight conditions. Successful microphone array measurements were also taken providing both acoustic source maps on the model, and quantitative spectra. Critical directivity measurements were obtained in the QFF. NASA Langley unstructured and structured Reynolds-Averaged Navier-Stokes codes modeled the steady aspects of the flows. Excellent comparisons with surface and off-surface experimental data were obtained. Subsequently, these meanflow calculations were utilized in both linear stability and direct numerical simulations of the flow fields to calculate unsteady surface pressures and farfield acoustic spectra. Accurate calculations were critical in obtaining not only noise source characteristics, but shear layer correction data as well. Techniques utilized in these investigations as well as brief overviews of the results are given.

Introduction

The importance of reducing airframe noise from subsonic airfraft in approach has now become apparent to the international community.[1] Civil air traffic continues to increase as does pressure from the public to control the resulting increase in landing noise which is particularly annoying to those living in close proximity to airports. It is clear that noise reduction technology is critical to the future development and operation of the world's air transportation system.

In response to the need for acceleration and augmentation in key subsonic technologies, NASA initiated the Advanced Subsonic Technology (AST) Program in Fiscal Year (FY) 1992. The NASA Noise Reduction Program began in FY 1994 under the AST Program and incorporated several key high payoff areas critical to the development of a new generation of environmentally compatible aircraft.[1] The Noise Reduction Program established a goal of a 10dB community noise impact reduction relative to 1992 subsonic transport technology. The goal will be achieved by combined noise reduction improvements in the engine system, the aircraft, and its operations. In FY95 the Noise Reduction Program began an intense effort in airframe noise source reduction and this research is the focus of this report. NASA also has a newly instituted base research program in airframe noise under the Advanced Concepts to Test (ASCOT) initiative. All these efforts will be critical in achieving the environmental goals set by NASA Administrator Daniel S. Goldin "to reduce the perceived noise levels of future aircraft by a factor of two from today's subsonic aircraft and by a factor of four within 20 years."[2]

NASA's airframe noise effort under the AST Noise Reduction Program involves partners in industry and academia. NASA Langley Research Center's (LaRC) role is to determine fundamental noise source mechanisms by relating sound generation mechanisms to fundamental

fluid mechanics. This is a critical need of our industry partners, since past predictions are largely based on empirical data that no longer suit the newer classes of aircraft. LaRC couples its building block experiments and computations to full configuration and large-scale tests carried out at NASA Ames Research Center (ARC) as well as flight data made available by Boeing. In addition, Lockheed Martin is a third partner performing computational aeroacoustics for experimentally defined sources. LaRC's effort to understand the flap-edge noise source began in 1995. Slat studies were initiated in 1997. The first landing gear experiments were performed in 1999. Work in all three areas is ongoing. Our objective is to obtain direct information regarding the actual noise generation mechanisms responsible for the spectrum produced by the flowfield.

The rest of the paper is organized as follows. The technical approach is presented as well as some information about the tools used to identify the important noise sources. Next, experimental and computational observations of flap-edge noise are addressed. Finally, some recent studies of trailing-edge and slat noise are reviewed. All of the examples demonstrate how experiment and computation have been used synergistically to identify important physical mechanisms behind important noise sources.

Technical Approach: Components

Since the mid-70's, researchers have found that the primary airframe noise sources emanate from the high-lift system and undercarriage of subsonic aircraft.[3,4] Depending on the type of aircraft, the dominant source vacillates between flap, slat and gear. Since none of these components are designed with aeroacoustics in mind, it is not surprising that their very structure gives rise to noise. In an effort to begin a thorough study of these complicated sources, a systematic investigation was initiated at NASA LaRC to look at the details of the meanflow surrounding these aircraft structures. Components (i.e., flap and slat) were first tested in isolation with simple models that gave rise to the same dominant acoustic source maps that were seen in full configuration tests and at larger scale. The models investigated were 3-element, unswept, partial span flap configurations. In both the flap and slat flowfields large-scale coherent structures were seen to dominate the flowfield. Details of these complicated vortical and separated flow systems were investigated with advanced experimental and computational tools giving rise to finer scale studies of the fluid mechanics and acoustics which could potentially play a role in airframe noise generation.

Following detailed investigations of the steady flowfield both experimentally (on- and off-surface data)[5] and computationally (Reynolds-Averaged Navier-Stokes),[6,7] flowfield fluctuations were measured using hot wires and hot films. The steady flowfield was also investigated for sources of unsteadiness using perturbation numerical simulations about the RANS base flow[8]. Linear stability theory helped pinpoint the dominant frequency ranges of unstable flow disturbances.[9] These efforts guided the correlation of acoustic measurements with proposed noise sources. Surface unsteady pressure measurements helped characterize the signature of the hydrodynamic fluctuations, and microphone array technology provided both quantitative spectra and farfield directivity.[10,11]

Maintaining a simplified model, tests were performed at flight Reynolds number to determine the variability of both the fluid mechanics and acoustics as this important parameter was increased. These tests, performed in NASA LaRC's Low Turbulence Pressure Tunnel (LTPT)[12] included a range of velocity sweeps at constant Reynolds number so that reliable scaling laws could be determined. Geometric modifications affecting conjectured fluid mechanic sources were tried so that cause and effect could be both understood and substantiated.

Flap-Edge Noise

Experimental Studies

Experimental investigations guided the more detailed computational work covered in a subsequent section. The most in-depth studies of both the fluid mechanics and acoustics of the flap-edge flowfield were conducted in the LaRC Quiet Flow Facility (QFF). The airfoil was a NACA 63_2 -215 Mod B wing (16-inch chord, 36 inch span) with a 30% chord half-span Fowler flap. This geometry was also tested in the NASA Ames 7x10 wind tunnel ,[13] a non-anechoic facility, which utilized a model of the same shape, but twice as large.

Initial investigations of the flap-edge flowfield involved laser light sheets and oil flows.[14] Laser light sheet images revealed a dominant vortex in the vicinity of the flap-edge. However, a short video constructed from the laser light sheet data did not reveal significant vibration of this structure (a noise generation mechanism originally conjectured). The signature of the vortex track on the flap edge surface was captured by oil flow applications on the pressure and suction side of the flap and main element. Fig. 1. shows these oil flow patterns.[5,14] The curved streamlines seen in both the suction and pressure surfaces give evidence of the flap-edge vortex. Although not seen in the figure, a smaller focus of streamlines on the flap side edge much closer to its trailing edge indicates the presence of a second, smaller vortex.

Further substantiation of the double vortex system are clearly seen in 5-hole probe studies performed in the QFF.[7] The measurements shown in Fig. 2 are normal planes of vorticity on the flap edge taken from these studies. The dual vortex system is clearly seen. The downstream planes indicate one dominant vortex resulting from the merger of the vortices. Note that at the trailing edge, the vortex is far removed from the flap surface.

Acoustic maps of high intensity noise on the flap side-edge closely mirror the fluid mechanics of the flow. Two microphone array systems were developed at NASA LaRC to quantify these results.[11] A large aperture array using 35 microphones was constructed to obtain high resolution noise maps. This array possesses a maximum diagonal aperture size of 34 inches. A unique logarithmic spiral layout design was chosen for the targeted frequency range of 2-30 kHz. In addition, a small aperture array, constructed to obtain spectra and directivity, complemented the larger design. This small array possesses 33 microphones with a maximum diagonal aperture size of 7.76 inches. It was easily moved in both azimuth and elevation about the model mounted in the QFF. Custom microphone shading algorithms have been developed to provide a frequency- and position-invariant sensing area from 10-40 kHz with an overall targeted frequency range for the array of 5-60 kHz. Both of these arrays were used with the NACA 63_2 -215 Mod B wing model described above. In Fig. 3., source localization maps from the large aperture array chart the progression of the hot spot for frequencies from 5 to 20kHz.[11] At the higher frequencies, this hot spot is localized on the edge of the flap. This is consistent with the primary vortex grazing the edge of the flap. As the frequency decreases the hot spot moves downstream and inboard, while the merged vortex system comes over the edge impinging on the upper surface. Recently reported noise reduction schemes by NASA Ames[15]indicate that flap-edge fences, which increase distance between the vortex system and the surface, can achieve noise reduction. The primary function of the fence is to prevent the vortex which starts on the flap edge from migrating to the upper surface. The fence acts as a dam, stopping the circulation around the edge from carrying the vortex on top of the flap. Fig. 4 compares pressure isosurfaces from computations with and without a flap fence. Clearly, in the case with a fence, the lower vortex remains on the edge. The fence is likely to cause more noise in the spanwise direction, but less noise under and above the wing.

A test conducted in the LaRC LTPT on a second model of a part-span flap was co-investigated by NASA's High-Lift Program element and LaRC's Airframe Noise team. This model, known as the Energy Efficient Transport (EET) model[16] has a vastly different cove design as well as camber on a flap optimized for high-lift. The LTPT test allowed Reynolds numbers to range from 3.6 to 19 million based on the chord. A further advantage of this pressure tunnel was the range of velocities achievable at constant Reynolds number, an important aspect for obtaining accurate scaling laws. This was the first test performed with an acoustic array at these high Reynolds number conditions. Array development[17] and data acquisition was performed by the Boeing Commercial Airplane Company. Although the primary acoustic sources present in the QFF/7x10 experiments appeared in the EET study, an additional hot spot at low frequency was also seen off the trailing edge of the flap. The acoustic image map indicating this additional source is given in Fig. 5b, in contrast with the map of the previously observed source shown in Fig. 5a. Details of the flowfield that corroborate this finding are discussed in the next section.

In virtually all studies conducted an abrupt rise in noise intensity occurred following an increase in flap deflection.[10,18] It was found both experimentally[5] and computationally[7] that both 29 and 39 deg. flap deflections also induced vortex bursting on the flap-edge system. The correlation of this event with noise is ongoing.

Computational Studies

An intensive investigation of the fluid dynamics associated with the high-lift system began in FY 1995. Mirroring the discussion above, these studies aimed at elucidating the flowfield surrounding the part span flap.

Initially, computations focused on the model tested in the QFF and 7x10 facilities. Validation of a Reynolds-Averaged Navier-Stokes solution is given in Fig. 6 from structured[6,7] and unstructured codes.[19,20] Depicted are Cp profiles on the main element and flap obtained in the 7x10 experiment compared against several of these computations. Most of the studies were performed using CFL3D on a structured mesh utilizing the Spalart-Allmaras turbulence model. An excellent comparison of Pressure Sensitive Paint (PSP) and computations of the vortex signature on the suction surface of the flap are given in Fig. 7.[7] PSP was the key measurement technique for obtaining details on the edge of the flap, and was used to validate the computational findings. However, oil flow methods were utilized on the flap edge[14] surface as well. Figure 8 compares oil flows and computational streamlines for a highly loaded flap setting. Note the accumulation of oil at approximately 2/3 chord. The separation and attachment lines abruptly end in this focal point. The computations clearly show that downstream of this point the flow reverses and moves upstream.[7] The most dramatic proof of the vortex bursting which gave rise to this focal point, occurred when Particle Image Velocimetry (PIV) was performed in the LaRC Basic Aerodynamic Research Tunnel.[21] Remarkable agreement with the calculations was obtained. Fig. 9 depicts streamwise velocity plots from RANS and PIV. Note the large region of reversed flow where the vortex lifts off the surface while undergoing bursting.

The above studies led to a series of systematic investigations utilizing the RANS solution as the model meanflow for both linearized stability studies[9] and temporal simulations.[8,22] Linear stability analyses identified frequency ranges with the highest growth rates. Numerical simulations indicated that these frequency ranges also had the most explosive growth. The latter calculations were interfaced with the Lighthill Acoustic Analogy, obtaining the first noise calculations for this complicated geometry.[22] The hot spots obtained in the QFF seemed to be explainable in terms of both cylindrical shear layer and vortical instabilities as discussed in references 8,9 and 22. Fig. 10 shows clearly the strong disturbance vorticity present in the shear layer that rolls into the flap-edge vortex. The results were calculated from a temporal DNS utilizing a normal cut of the part-span flap RANS solution at approximately 50% chord. The broadband nature of this instability becomes apparent, as this disturbance remains significant from 5 to 30 kHz. However, at the lower frequencies the vortex instability appears to be stronger than that of the shear layer. Recall from Fig. 3 that the 5kHz noise map indicates the maximum in intensity occurring inboard of the flap-edge at the location where the vortex moves rapidly over the edge and onto the suction surface (Fig. 2). The higher frequency noise maps in this figure indicate maxima more along the edge where the shear-layer instabilities should be dominant; this is confirmed in the above DNS and linear stability studies. The reader is referred to references 8 and 22 for more detail.

As alluded to in the previous section another source appeared during acoustic measurements on a second part-span flap model, the EET. Recall Fig. 5, which indicates a high noise region just off the trailing edge of the flap at low frequency. When the RANS solution was obtained for the EET geometry, a dramatic difference in vortex trajectory was discovered, relative to that seen in the 63_2 -215 flowfield. Fig. 11a shows planes of vorticity along the flap-edge of this model. If one contrasts these cuts with that of the 63_2 -215 flowfield (Fig. 11b) the vortex is seen to stay in close proximity to the edge surface of the flap down to the trailing edge for the EET flowfield. In contrast, the 63_2 -215 model flowfield has the vortex abruptly leaving the surface by around 60% chord. By the time the flow reaches the trailing edge in that case, the vortex is far-removed from any solid surfaces. It is believed that fluctuations in the vortex, being much nearer to the flap surface and trailing edge

for the EET model, potentially give rise to the additional hot spot of Fig. 5. Again, the acoustic signatures closely mirror the findings of the fluid mechanics.

Trailing-Edge Scattering

In addition to the linear DNS approach that has been very useful in the study of flap-edge noise, several other approaches have been successfully applied by the airframe noise team. Another hybrid approach employing a standard CFD solver and the Ffowcs Williams and Hawkings equation was recently validated for problems involving trailing-edge scattering. Calculation methods for acoustic fields that include trailing-edge noise currently are largely empirical.[23] Singer *et al*.[24] investigated the feasibility of directly computing the acoustic field generated by flow over a sharp trailing edge. A hybrid computational approach was taken wherein the CFL3D solver was used to accurately calculate the unsteady fluid dynamics over a relatively small region near the surface, and an acoustics code based on the Ffowcs Williams and Hawkings[25] (FWH) equation computed the acoustic field generated by the previously calculated unsteady near flow field. To investigate edge scattering, an airfoil with vortices convecting past its trailing edge was simulated. A 2.6% thickness NACA 00 series airfoil was placed in a flow with a small, flat plate introduced perpendicular to the flow at 98% chord. In the presence of flow, vortices roll up just downstream of the flat plate, alternately near the plate's top and bottom edges.

Figure 12 shows vorticity magnitude contours in the vicinity of the trailing edge at a single time step. The circular concentrations of vorticity indicate the individual vortices that constitute the unsteady Karman vortex street downstream of the vortex-generator plate. Cases were run with Mach numbers ranging from 0.2 to 0.5 that produced regular Strouhal shedding at the plate. The frequency of the vortices convecting past the trailing edge is less distinct because the vortices shed from the vortex-generator plate often pair and interact with neighboring vortices, as seen in Fig. 12.

The FWH code computed the acoustic field generated by the unsteady aerodynamic flow field. The far-field signals were obtained at several observer locations. Figure 13(a) shows spectra of the acoustic signals for several observer positions. The angular measurements are denoted as increasing for counterclockwise rotations, with 0 degrees being directed downstream. The figure shows greatly reduced noise radiation directly upstream and directly downstream. Integration of each acoustic spectrum over the frequencies provides the mean square acoustic pressure. Variation of the mean square acoustic pressure as a function of Mach number is plotted in Fig. 13(b). The symbols show the data, and the lines are linear least-squares fits to the logarithm of the data. For an observer at 30 degrees, the mean square pressure varies as the 5.2 power of Mach number. The theoretical formula for the variation of trailing-edge noise with Mach number requires an estimate of the rms fluctuating velocity in the vicinity of the edge. In most of the literature, the fluctuating velocity is assumed to vary linearly with the freestream Mach number. However, in this particular flow, the measured variation is $M^{1.34}$. Accounting for the actual rms fluctuating velocity in the calculations, a theoretical scaling of $M^{5.36}$ is implied, which is in close agreement with the computationally observed scaling of $M^{5.2}$. These computations have helped to verify that the hybrid approach is valid and capable of accurately predicting fairly complicated, broadband, acoustic phenomena.

Slat Noise

A cooperative test involving NASA's High-Lift Program Element and NASA's Airframe Noise Team was conducted in the LTPT to investigate slat noise. The EET model tested includes a full-span leading-edge slat and a part-span trailing flap. To obtain acoustic data, members of Boeing Commercial Airplane Company designed and built a microphone array that was installed in the wind tunnel. The microphone array and the subsequent data processing followed techniques developed earlier at Boeing.[17]

Figure 14(a) illustrates one unexpected feature of the experimental data. For a slat deflection of δ_s=30 degrees, a very large amplitude peak was observed in the acoustic spectrum in the vicinity of 50 kHz. This peak rises almost 20 dB above the signal observed for the case in which the slat is deflected 20 degrees.

During the course of the experiment, efforts to eliminate the high-frequency peak by altering the overhang of the slat were largely unsuccessful. Only for cases in which the overhang became unrealistically large was a significant change in the high-frequency acoustic peak observed. Increasing the configuration's angle-of-attack from 10 to 15 degrees, reduced the amplitude of the high-frequency peak by approximately 10 dB. For some time, no consistent explanation of the observed phenomena was available.

Khorrami *et al*.[26] provides details of unsteady, two-dimensional (2D), Reynolds-averaged Navier-Stokes (RANS) calculations designed to mimic the experimental conditions. In particular, the RANS computation was specially designed to properly incorporate and resolve the small, but finite trailing-edge thickness of the slat. Extremely small grid cells were used in the vicinity of the slat trailing edge and the time step was chosen to ensure more than 120 time steps per period of a 50 kHz signal. Slat deflections of both 30 and 20 degrees were simulated. These calculations clearly show vortex shedding from the slat trailing edge for the case with a 30 degree slat deflection. Figure 14(b) shows a snapshot of the pressure fluctuations produced in the flow field. The vortex shedding virtually disappears for the case of a 20 degree slat deflection.

Singer *et al*.[27] discuss the aeroacoustic analysis of the unsteady data. As a first approximation, the code developed by Lockard[28] for computing the 2D acoustic field from 2D CFD data was used to predict the sound field. Figure 15(a) shows computed spectra based on $1/12^{th}$ octave bands for an observer located at 270 degrees. Clearly the computed noise also has a significant peak in the spectra in the same frequency range as the experiment. This confirmed that the fluctuations from the slat vortex shedding weren't just hydrodynamic fluctuations, but also produced noise. Although the acoustic array used in the experiment was not intended to provide any directivity information, the high-frequency acoustic signal was so loud that it overwhelmed the intrinsic wind-tunnel noise and can be identified from the spectrum of some of the individual microphones used in the acoustic array. The relative amplitudes of the mean square fluctuating pressure in a frequency range around 50 kHz from a subset of microphones having approximately the same cross-stream location are compared with computed values in Fig. 15(b). The maximum amplitude of the microphone data is scaled with the maximum amplitude of the calculation. The non-zero microphone response far-upstream is associated with the wall-pressure fluctuations of the turbulent boundary layer along the wind-tunnel ceiling. These fluctuations are not included as part of the CFD calculations. Slightly upstream of the slat leading edge, the noise level rises. The maximum amplitude occurs in the mid-chord region followed by a sharp drop in amplitude. The qualitative features of the computations agree remarkably well with the microphone data, and the directivity results aided in the redesign of the acoustic array for a subsequent wind-tunnel test.

Conclusions

This work is part of a larger effort in the NASA AST Noise Reduction Program, which includes large scale testing at NASA Ames and Boeing Commercial Airplane Company as well as computational aeroacoustics performed at Lockheed Martin. Fundamental studies of airframe noise sources for subsonic aircraft are being conducted at NASA Langley Research Center. The work presented deals with the noise generated by the flap-edge and slat flowfields. A series of detailed experimental and computational building block studies were described corroborating several key noise source mechanisms associated with these important components. Coordination of acoustic source maps with Reynolds-Averaged Navier-Stokes solutions, linear stability analyses, and numerical simulations gave rise to plausible noise generation mechanisms stemming from both a cylindrical shear layer and a primary vortex structure on the flap and trailing-edge shedding from the slat. Newly designed array technology allowed for high Reynolds number testing in a hard wall facility, along with more detailed quantitative acoustic measurements in an anechoic chamber. Calculations of highly accurate mean flows as well as unsteady flow characteristics gave excellent agreement with both fluid mechanics and acoustic experiments of several part-span flap models.

Acknowledgements

The authors would like to thank William Willshire, Program Manager of the Noise Reduction Program for supporting the work presented. Special thanks to the exceptional team of airframe noise researchers responsible for results given: Dr. K. Brentner, Dr. T. Brooks, Dr. W. Humphreys, Dr. M. Khorrami, Professor Geoffrey Lilley, Dr. C. Gerhold, Dr. K. Meadows, Dr. R. Radeztsky, Dr. W. Hunter, Dr. B. Singer, Dr. M. Takallu, M. Sanetrik Dr. W. Anderson, J. Underbrink, Dr. R. Stoker, and G. Neubert.

References

1. Willshire, W.L. and Stephens, D.G.: "Aircraft Noise Technology for the 21st Century", NOISECON 98.
2. Goldin, Daniel S.: "Turning Goals into Reality," presented at World Aviation Congress, Los Angeles, CA, Oct. 15, 1997.
3. Crighton, D.G.: "Airframe Noise in Aeronautics of Flight Vehicles: Theory and Practice," Vol. 1; Noise Sources, NASA RP 1258, pp. 391-447, 1991.
4. Sen, R.: "A Study of Unsteady Fields Near Leading-edge Slats," AIAA 97-1696, 1997.
5. Radezrsky, R.H., Singer, B.A., and Khorrami, M.R.: "Detailed Measurements of a Flap Side-Edge Flow Field," AIAA 98-0700, 1998.
6. Takallu, M.A., and Laflin, K.R.: "Reynolds-Averaged Navier-Stokes Simulations of Two Partial-Span Flap Wing Experiments," AIAA 98-0701, 1998.
7. Khorrami, M.R., Singer, B.A. and Radeztsky, R.H.: "Reynolds Averaged Navier-Stokes Computations of a Flap Side-Edge Flow Field," AIAA 98-0768, 1998.
8. Streett, C.L.: Numerical Simulation of Fluctuations Leading to Noise in a Flap-Edge Flowfield," AIAA 98-0628, 1998.
9. Khorrami, M.R., and Singer, B.A.: "Stability Analysis for Noise-Source Modeling of a Part-Span Flap," AIAA 98-2225, 1998.
10. Meadows, K.R., Brooks, T.F., Gerhold, C.H., Humphreys, W.M . and Hunter, W.W.: Acoustic and Unsteady Surface Pressure Measurements of a Main Element-Flap Configuration," AIAA-97-1595.
11. Humphreys, W.M., Brooks, T.F., Hunter, W.W., and Meadows, K.R.: "Design and Use of Microphone Arrays for Aeroacoustic Measurements," AIAA 98-0471, 1998.
12. McGhee, R.J., Beasley, W.D., and Foster, J. M.: "Recent Modifications and Calibration of the Langley Low-Turbulence-Pressure-Tunnel," NASA TP-2328, 1984.
13. Storms, B.L., Takahashi, T.T., and Ross, J.C.: "Aerodynamic Influence of a Finite-Span Flap on a Simple Wing," SAE Paper 951977, 1995.
14. Experiment performed by Barry Lazos at NASA Langley Research Center.
15. Horne, C.F., Hayes, J., and Ross, J.C.: "Measurements of Unsteady Pressure Fluctuations on the Surface of an Unswept Multi-Element Airfoil," AIAA 97-1645, 1997.
16. Morgan, H.L., Jr.: "Model Geometry Description and Pressure Distribution Data from Tests of EET High-Lift Research Model Equipped with Full-Span Slat and Part-Span Flaps," NASA TM-80048, 1979.
17. Underbrink, J.R. and Dougherty, R.P.: "Array Design for Non-intrusive Measurements of Noise Sources," NOISECON 96, 1996.
18. Hayes, J.A., Horne, C.W., and Bent, P.H.: "Airframe Noise Characteristics of a 4.7% Scale DC-10 Model," AIAA-97-1594-CP, 1997.
19. Anderson, W.K., Rausch, R.D. and Bonhaus, D.L.: "Implicit/Multigrid Algorithms for Incompressible Turbulent Flows on Unstructured Grids," Journal of Computational Physics, vol. 128, pp. 391-408, 1996.
20. Mavriplis, D.J., and Venkatakrishnan, V.: "A Unified Solver for Navier-Stokes Equations on Mixed Element Meshes," International Journal for Computational Fluid Dynamics," vol. 8, pp. 247-263, 1997.
21. PIV measurements performed in the NASA LaRC BART facility by L. Jenkins, P. Yao, and K. Paschal.
22. Streett, C.L.: "Numerical Simulation of a Flap-Edge Flowfield," AIAA 98-2226, 1998.
23. Wagner, S., Bareiss, R. and Guidati, G., Wind Turbine Noise Springer, New York, 1996.
24. Singer, B. A., Brentner, K. S., Lockard, D. L. and Lilley, G. M., "Simulation of Acoustic Scattering from a Trailing Edge," AIAA 99-0231, January 1999.

25. Ffowcs Williams, J. E. and Hawkings, D. L., "Sound Generated by Turbulence and Surfaces in Arbitrary Motion," Philosophical Transactions of the Royal Society, A264, 1151, pp. 321-342. 1969.
26. Khorrami, M. R. and Berkman, M. E. and Choudhari, M.and Singer, B. A. and Lockard, D. L. and Brentner, K. S., "Unsteady Flow Computations of a Slat with a Blunt TrailingEdge," AIAA 99-1805, May, 1999.
27. Singer, B. A. and Lockard, D. L. and Brentner,K. S. and Khorrami, M. R. and Berkman, M. E. and Choudhari, M., "Computational Acoustic Analysis of Slat Trailing-Edge Flow," AIAA 99-1802, 1999.
28. Lockard, D. P., An Efficient, "Two-Dimensional Implementation of the Ffowcs Williams and Hawkings Equation," to appear in Journal of Sound and Vibration.

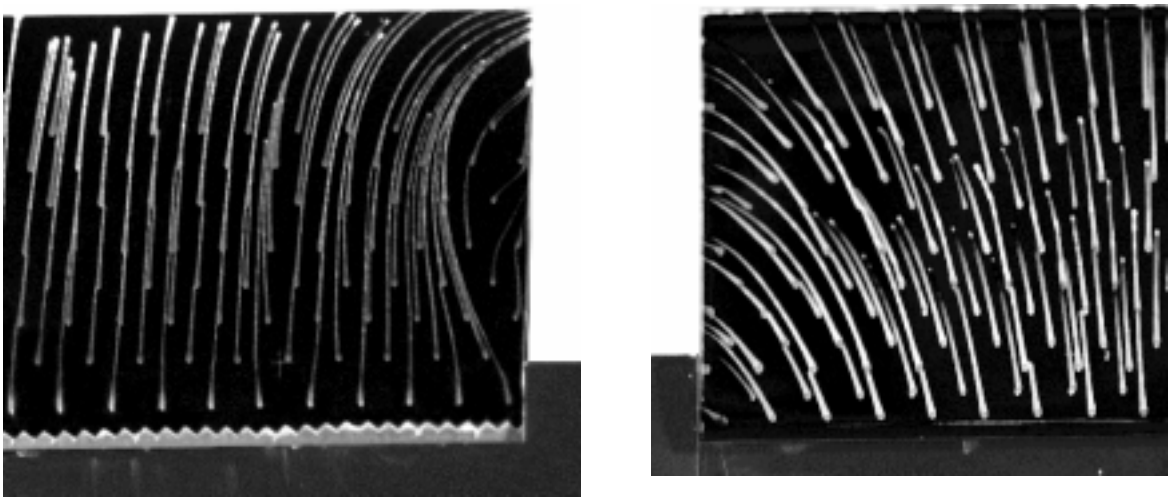

a) suction surface **b) pressure surface**

Figure 1. Oil flow patterns on the flap-edge of the 63_2-215 Mod B wing.

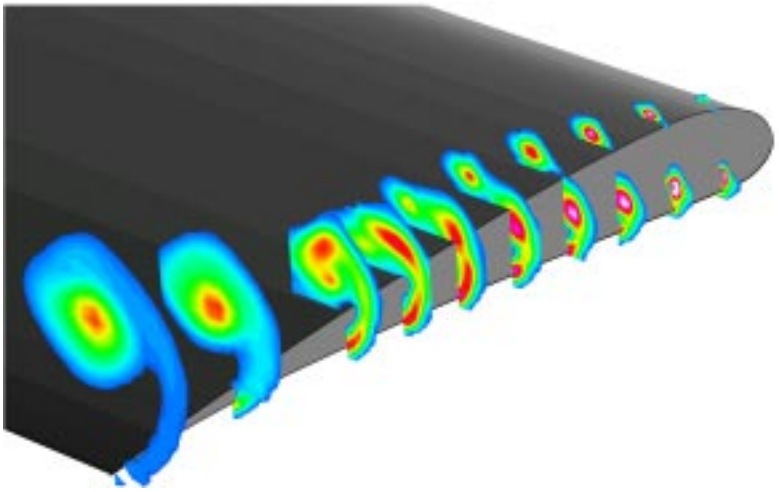

Figure 2. Five hole probe contours of streamwise vorticity at the flap-edge.

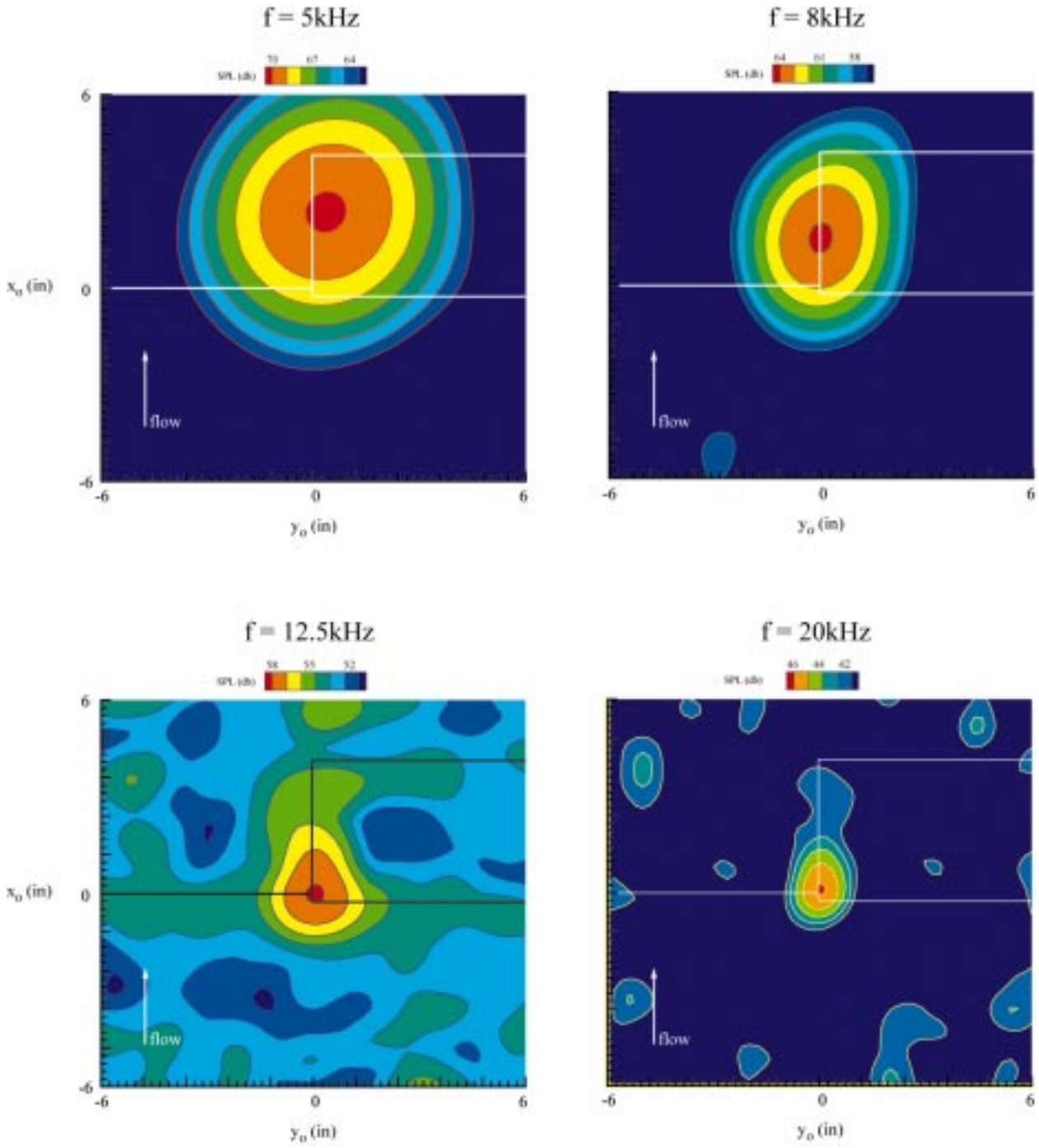

Figure 3. Sound source localization maps from acoustic array measurements in the Quiet Flow Facility.

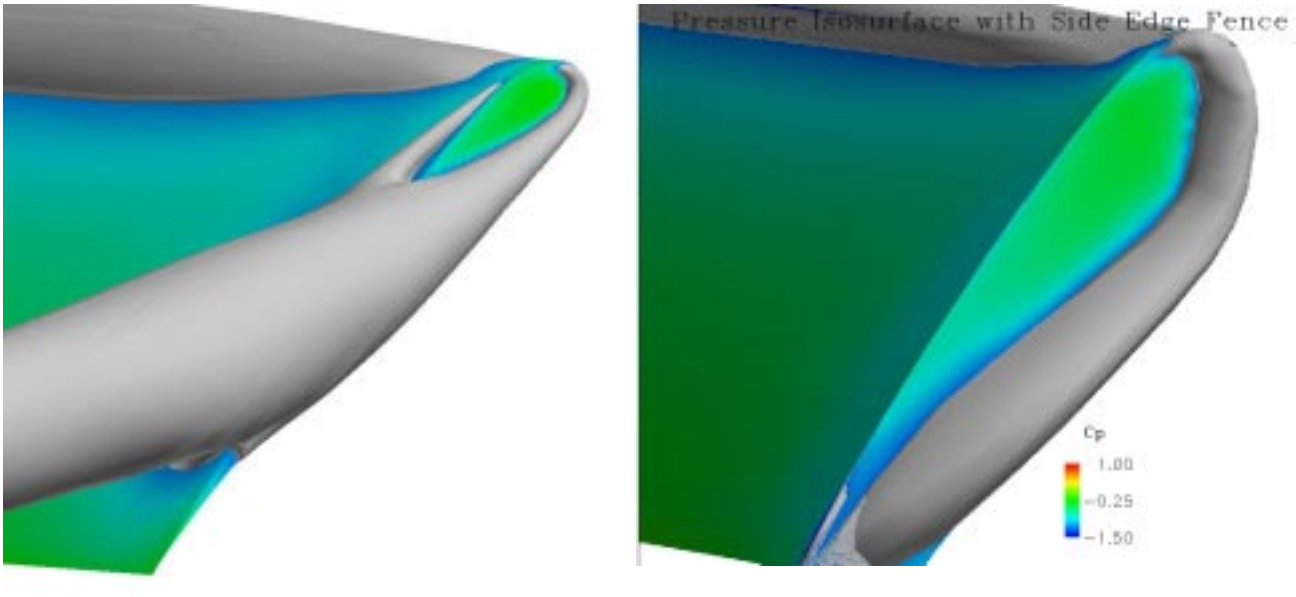

a) Without flap fence **b) With flap fence**

Figure 4. Pressure Isosurfaces from calculations.

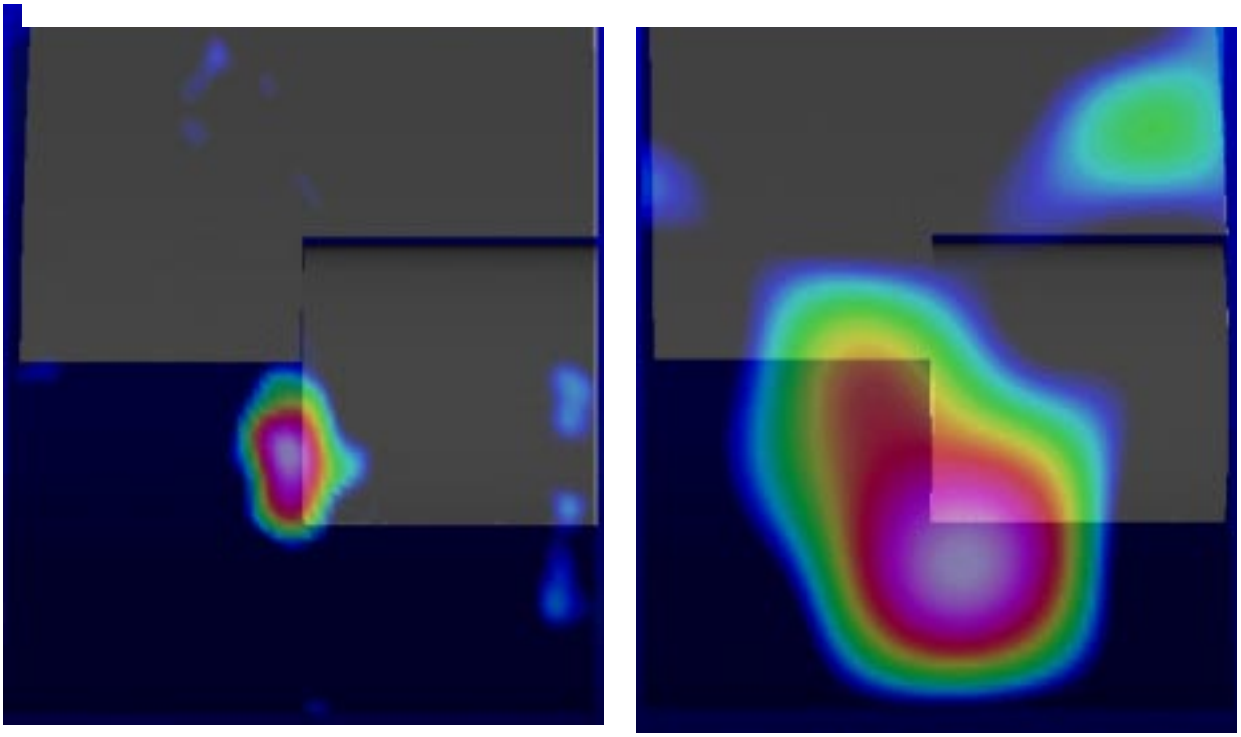

a) side-edge source (high frequency) **b) trailing-edge source (low frequency)**

Figure 5. Sound source localization map from EET part span model in the Low Turbulence Pressure Tunnel.

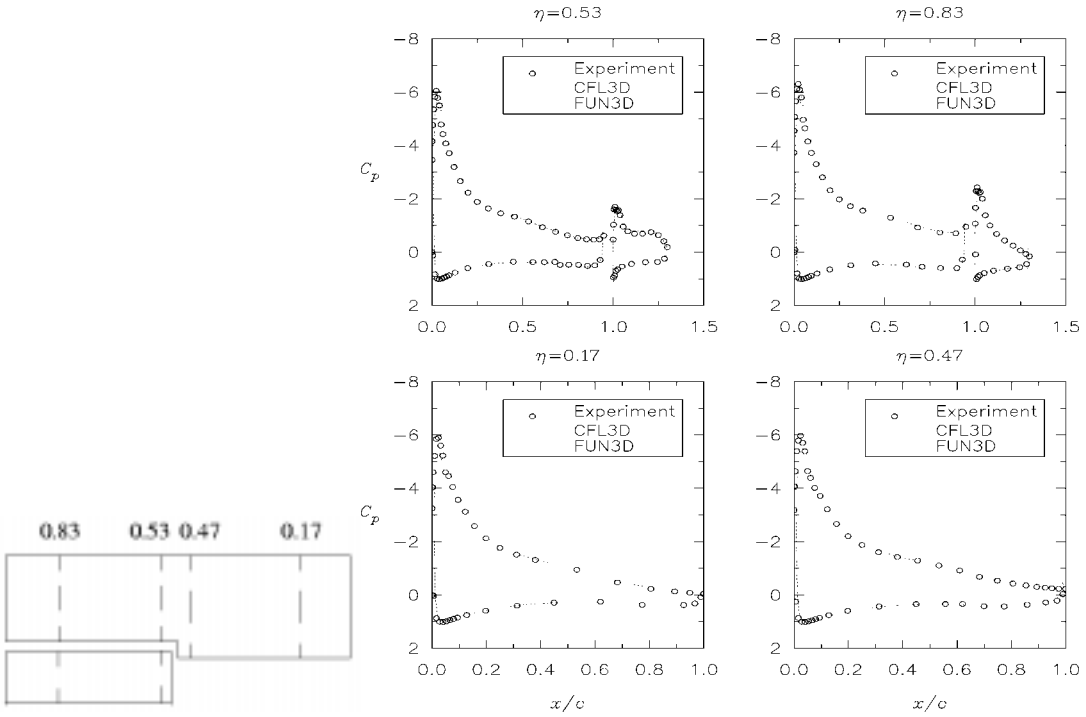

Figure 6. Experimental and computational Cp profiles from the 7x10 flap-edge test: CFL3D – structured, FUN3D - unstructured.

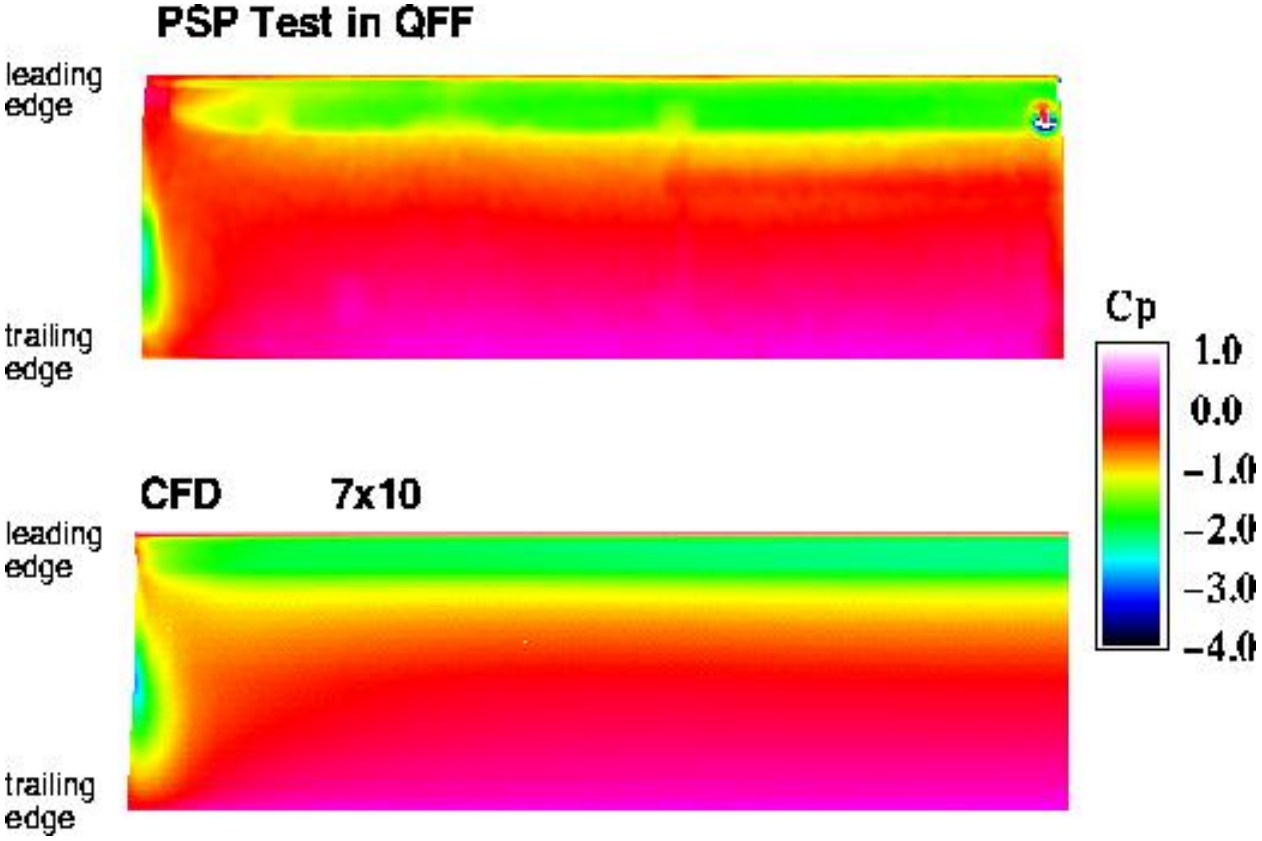

Figure 7. Comparison between computed and pressure sensitive paint measurements taken in the QFF on the suction surface of the flap.

a) experiment – oil flow

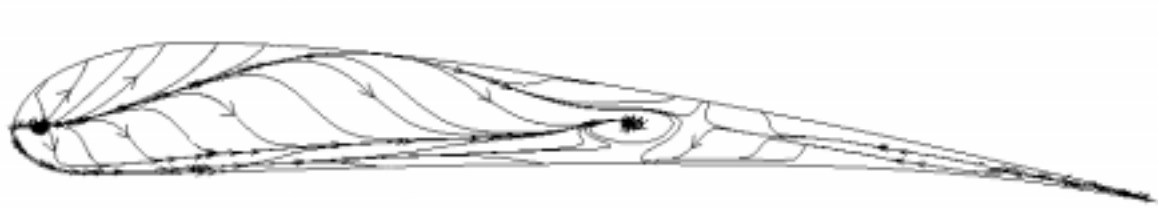

b) CFD – surface streamlines

Figure 8. Flap side-edge surface streamlines indicating focal point for flow reversal at high flap deflection.

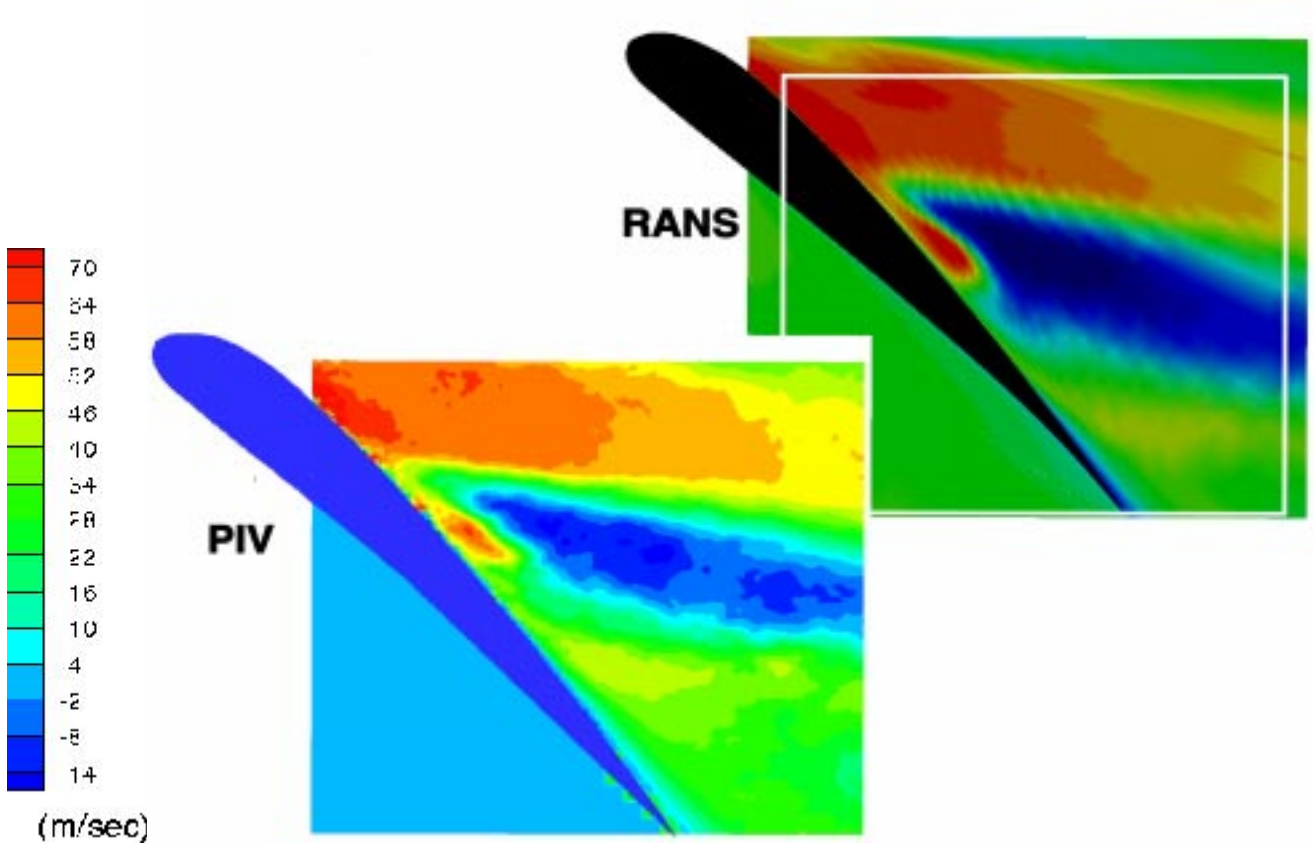

Figure 9. Streamwise velocity plots corroborating strong vortex bursting at high flap deflection: PIV and RANS comparison.

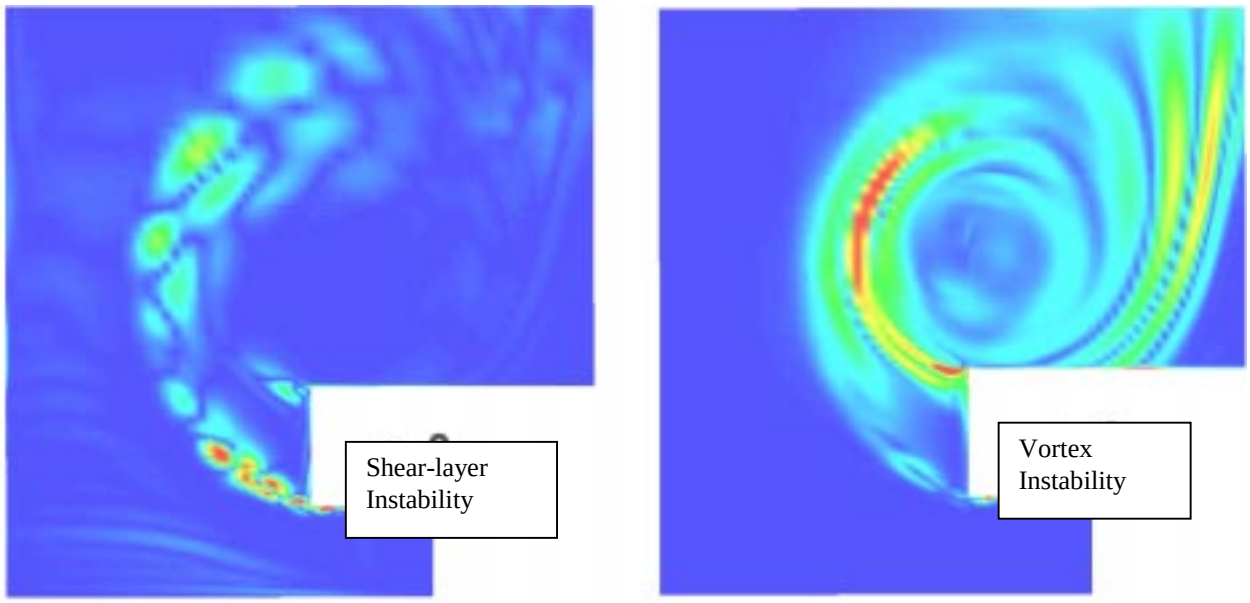

Figure 10. Calculated disturbance vorticity from shear-layer and vortex instabilities, from temporal DNS linearized about a normal cut of a Reynolds Averaged Navier-Stokes solution; 50% flap chord.

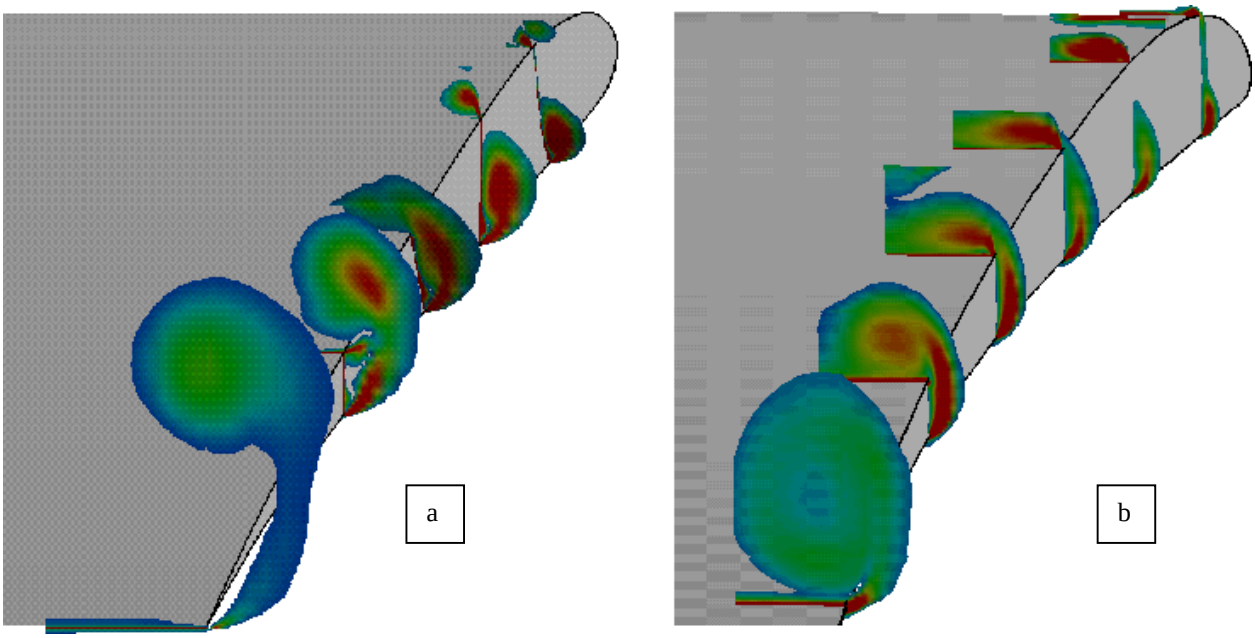

Figure 11. Comparison of streamwise vorticity contours on the flap side edge for two part-span flap models: a) NACA 63_2-215 (QFF/7x10 model); b) EET (LTPT model)

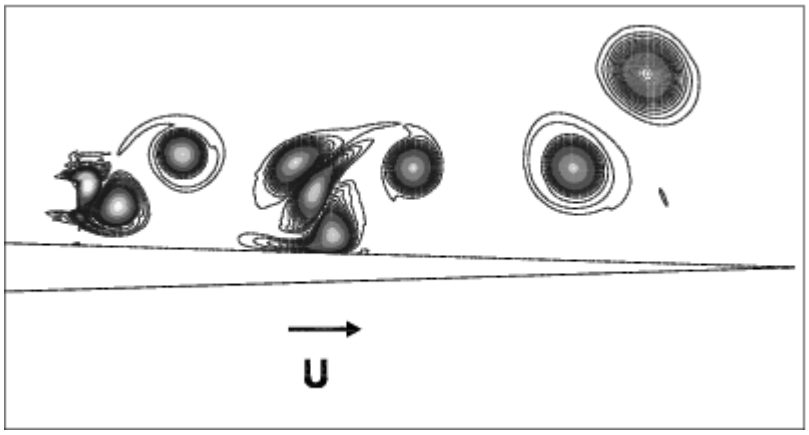

Figure 12. Instantaneous vorticity magnitude contours in vicinity of trailing edge for M=0.2 case. Approximately 2% of aft portion of airfoil is shown.

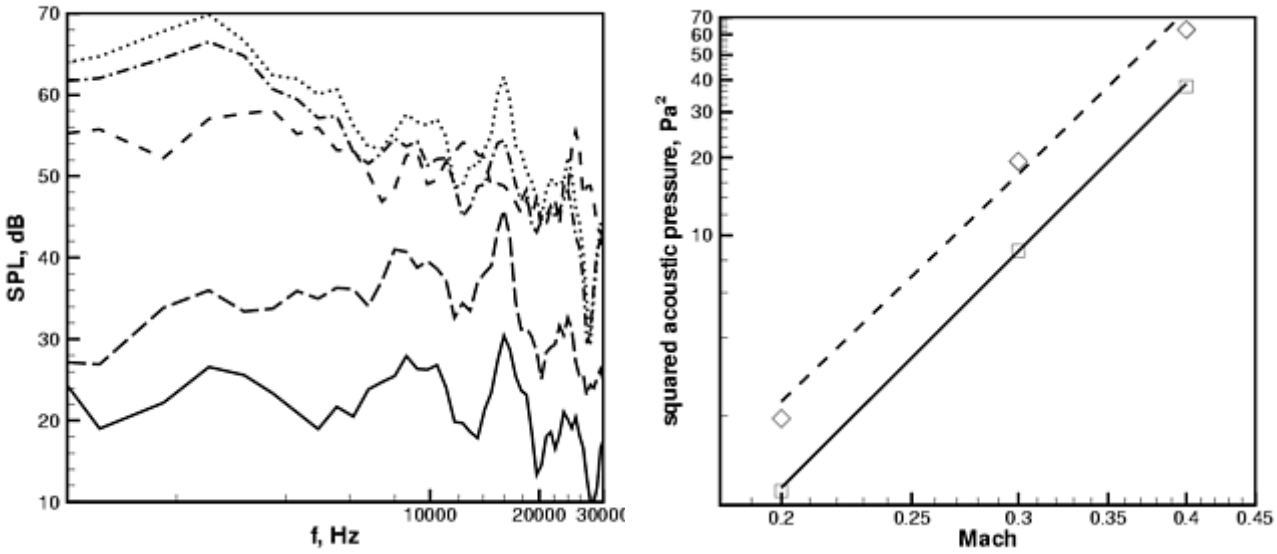

a) **b)**

Figure 13. (a) Spectra of acoustic signals (referenced to 20μPa) for observers located 10 C from trailing edge of airfoil; on-airfoil-body integration surface used, M=0.2. Observers located at: ——— 0 deg., – – – – 45 deg., –·–·–·– 90 deg., ····· 135 deg., — — — 180 deg. (b) Variation in mean square acoustic pressure versus Mach number; □ data for 30 deg., ——— least-squares fit for 30 deg., ◇ data for 45 deg., – – – – least-squares fit for 45 deg.

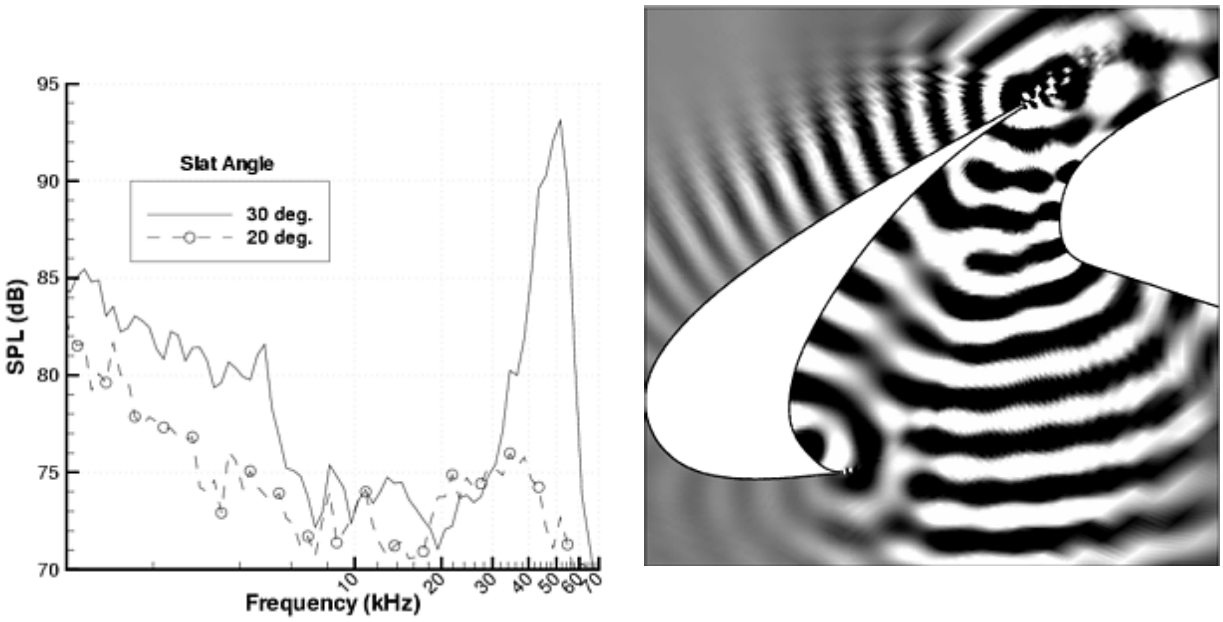

a) b)

Figure 14. (a) Acoustic spectrum based upon 1/12th octave bins with array focussed on slat region. Configuration angle of attack is 10 deg., Reynolds number is 7.2 million, Mach number is 0.2. (b) Instantaneous fluctuation pressure, in vicinity of leading-edge slat, from CFD calculation. Slat deflection is 30 deg.

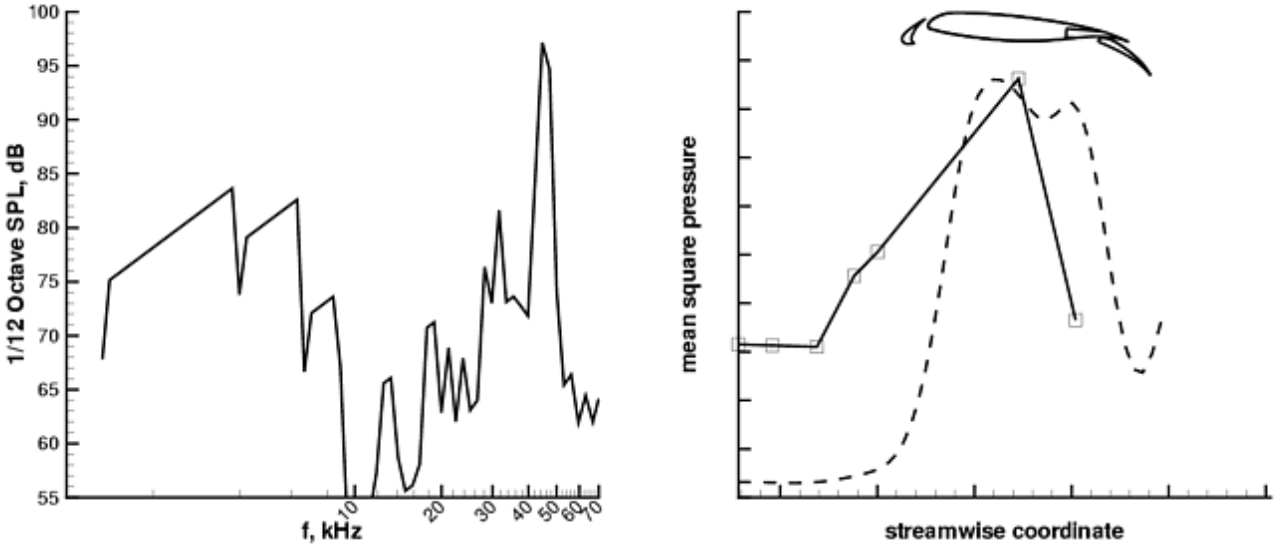

a) b)

Figure 15. (a) Spectra for observer positioned at 270 deg. with 30 deg. slat deflection. (b) Comparison of squared acoustic pressure at individual microphones to that predicted computationally. Microphone positions and values are shown with squares; dashed line indicates computationally predicted values.